Available online at www.sciencedirect.com
SCIENCE DIRECT®
Journal of Molecular Catalysis A: Chemical 223 (2004) 353–361
JOURNAL OF MOLECULAR CATALYSIS A: CHEMICAL
www.elsevier.com/locate/molcata

Characterization and catalytic properties of niobia supported nickel catalysts in the hydrodechlorination of 1,2,4-trichlorobenzene

Komandur V.R. Chary[a,*], Katar Sri Lakshmi[a], Pendyala Venkat Ramana Rao[a], Kamaraju Seetha Rama Rao[a], Maria Papadaki[b]

[a] *Catalysis Division, Indian Institute of Chemical Technology, Hyderabad 500007, India*
[b] *Chemical Engineering Department, The University of Leeds, Leeds LS29JT, UK*

Received 10 February 2003; received in revised form 24 August 2003; accepted 1 September 2003
Available online 21 September 2004

Abstract

A series of nickel (2–15 wt.%) catalysts supported on niobia were prepared. Their catalytic efficiency in the vapour phase hydrodechlorination of 1,2,4-trichlorobenzene was studied. The catalyst samples were characterized by X-ray diffraction (XRD), scanning electron microscopy (SEM), X-ray photoelectron spectroscopy (XPS), temperature programmed desorption of hydrogen (TPD), temperature programmed reduction (TPR) and hydrogen chemisorption method. Hydrogen chemisorption studies suggest that the hydrogen spillover culminates at 6 wt.% of Ni/Nb_2O_5. The partial hydrodechlorination ability of 6 wt.% Ni/Nb_2O_5 was also found to be the highest. Niobia supported nickel catalysts were found to be highly active for the partial hydrodechlorination of 1,2,4-trichlorobenzene. It was also found that the catalytic properties are related to dispersion of nickel on niobium oxide.

Keywords: Niobia; Hydrodechlorination; Spillover hydrogen; SMSI

1. Introduction

The gas phase catalytic hydrodechlorination of chlorinated and polychlorinated aromatic compounds is a far better method of treatment of organic wastes than the conventional ones like incineration. Catalytic hydrodechlorination [1–3] is now emerging as an alternative, economically viable process for more efficient, ecological treatments of chlorinated organic wastes [4,5]. Information on hydrodechlorination processes of complex polychlorinated aromatic compounds is difficult to find. Catalytic hydrodechlorination of organic halides produce the corresponding hydrocarbon and hydrogen chloride. The produced hydrogen chloride can be readily separated while the hydrocarbon can be recycled to minimize the waste. Niobium-based materials have been recently employed as catalysts in numerous catalytic applications. There are various functions of niobium compounds in heterogeneous catalysis [6]. Niobia can be used as a support, promoter and solid acid and is easily reducible over a wide temperature range. Niobia is also known as a typical strong metal support interacting (SMSI) oxide [7], Ko et al. [8] have reported that for hydrocarbons, the niobia supported nickel catalysts exhibited higher conversion and selectivity during Fischer–Tropsch synthesis than the nickel catalysts supported on alumina or silica. Nickel catalysts are extensively used in hydrogenation reactions but there are only few reports [1,4,9,10] regarding their application in hydrodechlorination reactions. In the present study we report for the first time some interesting results on the use of niobia supported nickel catalysts for hydrodechlorination of 1,2,4-trichlorobenzene.

2. Experimental

2.1. Catalyst preparation

Niobium(V) oxide was prepared by calcination of niobium pentoxide hydrate (Niobia HY-340, AD/1227, CBMM,

* Corresponding author. Tel.: +91 40 27193162; fax: +91 40 27160921.
E-mail address: kvrchary@iict.res.in (K.V.R. Chary).

1381-1169/$ – see front matter © 2004 Elsevier B.V. All rights reserved.
doi:10.1016/j.molcata.2003.09.049

Brazil) in air at 773 K for 5 h. Subsequently, a series of nickel catalysts (nickel loadings ranging from 2 to 15 wt.%) supported on niobium(V) oxide (surface area 55 $m^2\,g^{-1}$) were prepared by impregnation with an aqueous solution containing $Ni(NO_3)_2{\cdot}6H_2O$ (Fluka). The catalysts were subsequently dried at 383 K for 16 h and calcined in air at 773 K for 5 h.

3. Catalyst characterization

3.1. X-ray diffraction (XRD)

XRD patterns of pure Nb_2O_5 and Ni/Nb_2O_5 samples were recorded on Siemens D5000 X-ray diffractometer using nickel-filtered Cu Kα radiation.

3.2. Temperature programmed reduction

The catalysts were characterized by temperature programmed reduction (TPR), pulse hydrogen chemisorption and BET surface area measurements. The above experiments were conducted on AutoChem2910 (Micromeritics, USA) and the details of the instrument are given elsewhere [11]. Temperature programmed reduction was carried out on 100 mg of the catalyst sample using 5% H_2/Ar (50 ml min^{-1}) from ambient temperature to 1073 K at a heating rate of 10 K min^{-1}. Prior to TPR experiments the catalyst sample was pretreated with helium (50 ml min^{-1}) at 473 K for 2 h. The peak areas were quantified using reduction of silver oxide as a reference.

3.3. X-ray photo electron spectroscopy (XPS)

The XPS spectra of the calcined samples were obtained with a Kratos-Axis 165 spectrometer using magnesium anode at 75 W ($h\nu$ = 1253.6 ev). The spectra were analyzed in terms of relative intensities and chemical displacement of Nb and Ni. Charge correction for the powder samples was related to the C 1s peak at 284.6 ev. Calculations of the atomic ratios (Ni/Nb) were performed by determining the Nb ($3d_{5/2}$) and Ni ($2p_{3/2}$) peak areas, after subtracting the inelastic background and correction intensities multiplied by the respective sensitive factors.

3.4. Hydrogen chemisorption

Hydrogen chemisorption was measured by the pulse method to estimate dispersion of nickel on Nb_2O_5 support. Prior to hydrogen chemisorption measurements, approximately 350 mg of the sample was reduced in a flow of 10% H_2/Ar (30 ml min^{-1}) at 673 K for 2 h and subsequently flushed with argon (30 ml min^{-1}) at the same temperature for 1 h and then cooled down to ambient temperature. Hydrogen chemisorption was measured at room temperature by introducing pulses of 10% H_2/Ar in pure argon stream (30 ml min^{-1}) with calibrated loop doses. The doses were continued till no further uptake of hydrogen was observed.

3.5. Temperature programmed desorption of hydrogen

Temperature programmed desorption (TPD) studies were carried out on an AutoChem2910 (Micromeritics, USA). In a typical TPD experiment about 500 mg of the sample was taken in a U-shaped quartz sample tube supported on a quartz wool bed. The sample was reduced in a flow of hydrogen (50 ml min^{-1}) at a temperature of 673 K to remove all the physisorbed hydrogen for 40 min. The oven was heated from room temperature to 1073 K. The hydrogen concentration in the effluent stream was monitored with the thermal conductivity detector and the areas under the peaks were calculated using GRAMS/32 software.

3.6. Scanning electron microscopy (SEM)

Scanning electron micrographs are obtained with a JSM 5410 scanning electron microscope operating at an accelerating voltage of 15 kV and a work distance (WD) of 16 mm and magnification values in the range of 10,000–50,000×. This technique was used to study the morphology and measure the size of the NiO particles.

3.7. Catalytic experiments

A down flow fixed bed reactor operating at atmospheric pressure was used for testing the catalyst for hydrodechlorination of 1,2,4-trichlorobenzene. About 2 g of the catalyst, mixed with an equal amount of quartz spheres were placed into the reactor (2 cm internal diameter and 20 cm length) and were supported by a glass wool bed. Prior to introducing the reactant 1,2,4-trichlorobenzene with a syringe pump, the catalyst was reduced at 673 K for 3 h in hydrogen flow (60 ml min^{-1}). The catalytic measurements were made at an overall gas hourly space velocity of 50,205 h^{-1}. Each catalytic run was repeated four times using different samples from the same batch of the catalyst and the measured conversions did not deviate by more than 2–3%. The reaction was carried out at a temperature of 523 K for a period of 5 h, which is sufficient to get the steady state activity. The reactor effluent was frozen in a liquid nitrogen trap for subsequent analysis, which was made using HP5973 quadrupole GC-MSD system with a HP-1MS capillary column.

4. Results and discussion

4.1. X-ray diffraction (XRD)

The XRD patterns of pure Nb_2O_5 and Ni/Nb_2O_5 catalysts with varying nickel contents on the support are shown in Fig. 1. In all the Ni/Nb_2O_5 samples NiO peaks, indicated by an asterisk (*), appeared at d = 2.088 Å, (2θ = 43.3) along

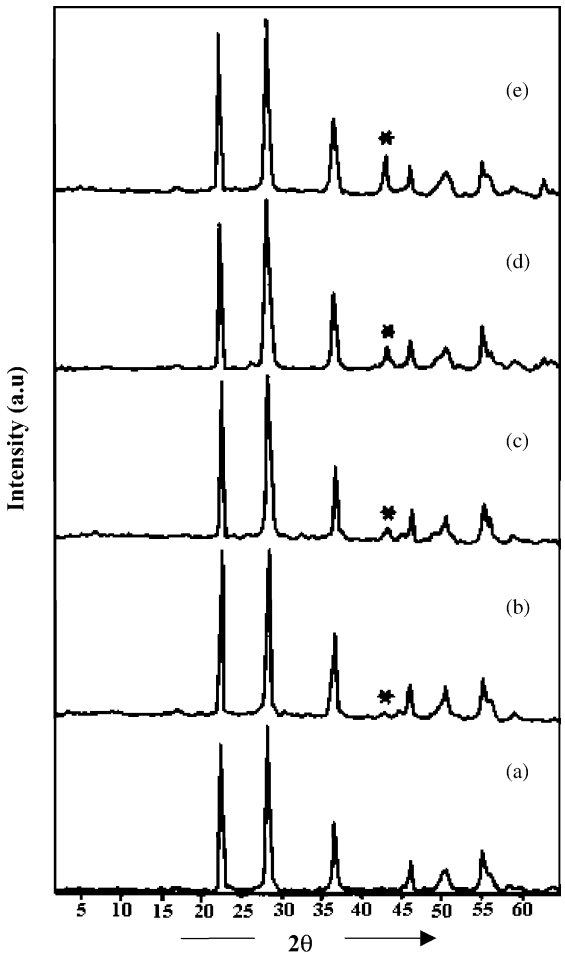

Fig. 1. XRD profiles of (a) pure Nb_2O_5, (b) 2 wt.% Ni/Nb_2O_5, (c) 6 wt.% Ni/Nb_2O_5, (d) 10 wt.% Ni/Nb_2O_5 and (e) 15 wt.% Ni/Nb_2O_5.

with the intense peaks of pure Nb_2O_5. The XRD of pure Nb_2O_5 (due to TT phase Nb_2O_5, a less crystalline form of T (T from the German "tief" for low) stabilized by impurities) is in agreement with the structure of Nb_2O_5 reported by Ko and Weissman [12]. This phase is the low temperature phase of Nb_2O_5 (it is formed at 773 K). The intensity of NiO peak increases with Ni loading on Nb_2O_5. The XRD patterns also reveal that there is no mixed oxide phase formed between NiO and Nb_2O_5.

4.2. Scanning electron microscopy (SEM)

The morphology of the samples was investigated by scanning electron microscopy. The micrographs show that the catalysts samples exhibited homogeneous NiO particles between 3000 and 5000 Å, are shown in Fig. 2. As the nickel loading increases there is an increase in the size of the NiO particles.

4.3. Temperature programmed reduction (TPR)

The temperature programmed reduction and chemisorption properties of various Ni/Nb_2O_5 catalysts are given in

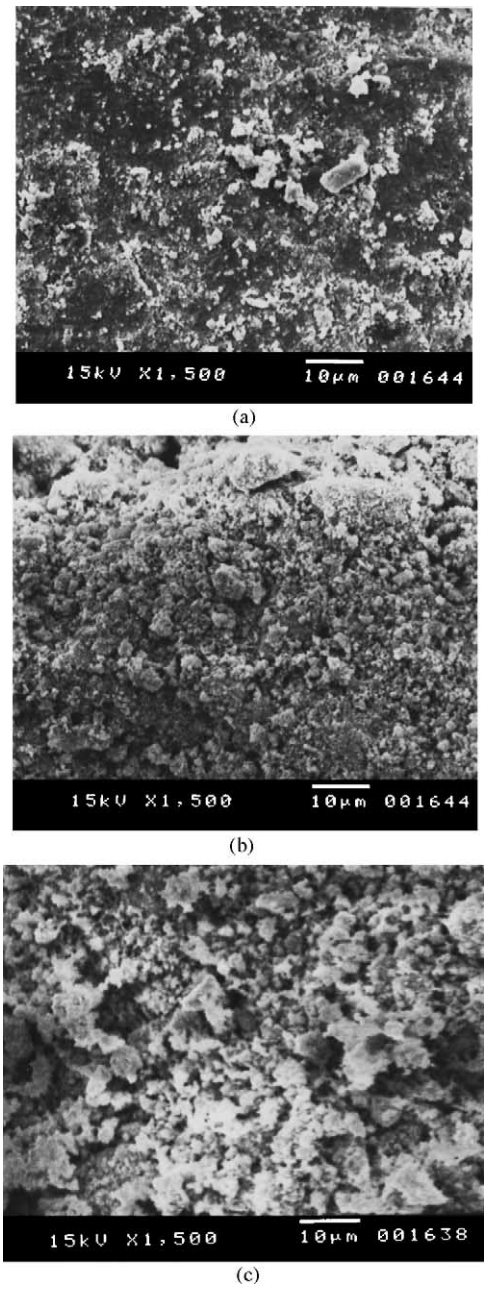

Fig. 2. SEM pictures of (a) 2 wt.% Ni/Nb_2O_5, (b) 10 wt.% Ni/Nb_2O_5 and (c) 15 wt.% Ni/Nb_2O_5.

Table 1. TPR profiles of various Ni/Nb_2O_5 and pure Nb_2O_5 are shown in Fig. 3. Pure Nb_2O_5 (Fig. 3a) has not shown any reduction peaks up to 1073 K. However, Ni/Nb_2O_5 samples have shown broad reduction peaks between 673 and 720 K, which are attributed to the reduction of Ni^{2+} to Ni^0. However from the results obtained from XPS we see peaks corresponding to NiO, Ni_2O_3 that is not the case in TPR because TPR is a bulk technique whereas XPS is a surface technique. From the same figure it can be seen that the intensity of the reduction peak increases with nickel loading. The T_{max} positions during TPR and hydrogen consumption results are reported in Table 1. As seen from this table, the hydrogen

Table 1
Results of BET surface area, temperature programmed reduction, hydrogen chemisorption and dispersion for various Ni/Nb_2O_5 catalysts

wt.% of Ni/Nb_2O_5	BET surface area ($m^2\ g^{-1}$)	T_{max} (K)	H_2 consumption[a] ($ml\ gcat^{-1}$)	H_2 uptake[b] ($\mu mol\ gcat^{-1}$)	% Dispersion [c]	TOF [d] $\times 10^{-2}$ (s^{-1})	Metal area ($m^2\ g^{-1}$)
2.0	50.0	720	7.29	7.67	4.50	6.0	0.6
6.0	44.6	755	26.5	9.37	1.83	7.4	0.73
10.0	40.8	673	40.3	8.97	1.05	5.5	0.70
15.0	29.2	670	58.3	11.5	0.90	5.3	0.90

[a] H_2 consumption obtained from TPR.
[b] H_2 uptake and metal area obtained from pulse hydrogen chemisorption, $T_{reduction}$ = 673 K.
[c] Dispersion = fraction of nickel atoms at the surface assuming H/Ni = 1.
[d] TOF = turn over frequency.

consumption during TPR also increases with nickel loading on niobia. The amount of hydrogen consumed during TPR for the reduction of the nickel exceeded the theoretical value due to spillover of hydrogen [13–17] from the metal to the support. This spillover is considerable in the case of 2 and 6 wt.% Ni/Nb_2O_5 sample but it was found to decrease with increasing Ni loading. It is interesting to note that the T_{max} during TPR (Table 1) also increases with nickel loading up to 6 wt.% Ni and decreases at higher nickel loading. The shift of T_{max} values with nickel loading might be due to the existence of strong metal support interaction (SMSI), which is also further reflected in catalytic properties of these catalysts.

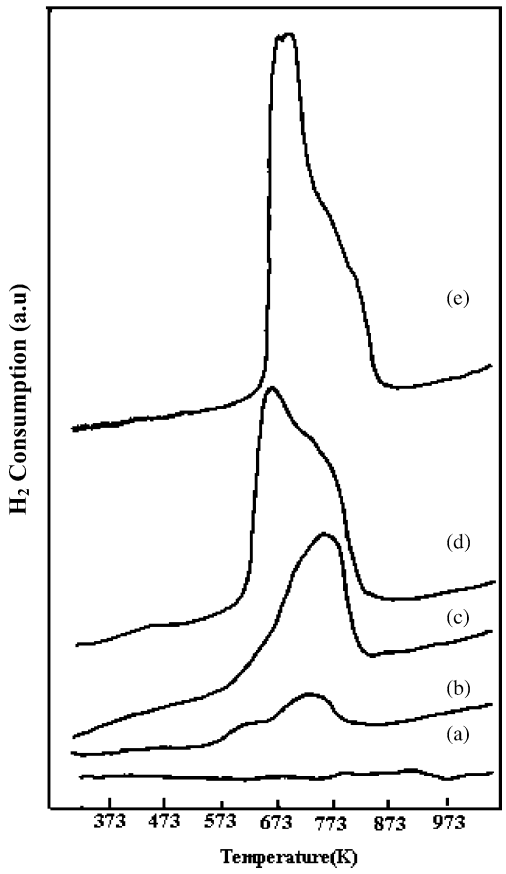

Fig. 3. TPR profiles of (a) pure Nb_2O_5, (b) 2 wt.% Ni/Nb_2O_5, (c) 6 wt.% Ni/Nb_2O_5, (d) 10 wt.% Ni/Nb_2O_5 and (e) 15 wt.% Ni/Nb_2O_5.

Keane [18] reported similar observations in TPR of Ni/SiO_2 catalysts.

4.4. Hydrogen chemisorption

Both, the BET surface area and the metal dispersion were found to decrease with increasing metal loading shown in Table 1. However, although the amount of chemisorbed hydrogen was significantly higher in the 6 wt.% Ni/Nb_2O_5, the nickel surface area of the same sample was found to be only marginally higher than the one of 10 wt.% Ni/Nb_2O_5 sample. This indicates that hydrogen is not only chemisorbed on nickel but is also taken by the niobia support. These results were thus attributed to the hydrogen spillover. Hydrogen spillover was found to decrease as the nickel loading increased above 6 wt.%. In recent past many researches [1–3,15,16,19] have investigated the influence of hydrogen chemisorption properties of nickel catalysts. Factors like reduction temperature, nature of reducing gas, flow rate; inert atmosphere and the duration of reduction might influence the hydrogen chemisorption properties of nickel catalysts.

4.5. Temperature programmed desorption of hydrogen

To obtain information about structural surface differences among several niobia supported nickel catalysts hydrogen TPD was performed. The number and approximate population of the various kinds of adsorbed species depend on many factors, the method of catalyst preparation, the kind of support, weight of the catalyst, flow rate of the carrier gas and the shape of the reactor system affect the conditions for the removal of desorbed hydrogen [3]. Fig. 4 shows the peaks observed on desorption of hydrogen for the catalysts samples. TPD curves for 2 wt.% catalyst sample show a low temperature broad peak at 371 K and a high temperature less intense peak at 763 K. The low temperature region below 625 K has been associated with different adsorption states of the hydrogen (presumably related to a different morphology and size of the nickel particles) for other supported nickel catalysts [20,21]. However a hydrogen spillover phenomenon is more likely to occur with the TPD peaks below 680 K [22,23]. Various authors have explained the appearance of high tem-

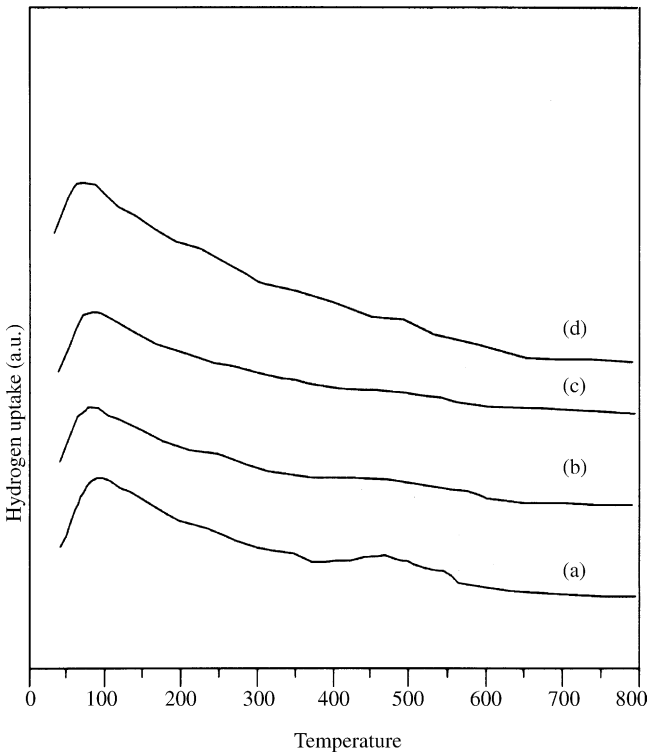

Fig. 4. TPD profiles of (a) 2 wt.% Ni/Nb_2O_5, (b) 6 wt.% Ni/Nb_2O_5, (c) 10 wt.% Ni/Nb_2O_5 and (d) 15 wt.% Ni/Nb_2O_5.

perature peaks due to the hydrogen spillover that takes place at the high temperature region during TPD runs [22,23].

4.6. X-ray photoelectron spectroscopy (XPS)

XPS spectra of the calcined Ni/Nb_2O_5 catalysts shown in Fig. 5 with varying nickel content shows two peaks (Ni $2p_{3/2}$) with E_b = 856.18, 855.16 and a satellite peak at E_b = 862 ev corresponding to NiO, Ni_2O_3 existing as Ni^{2+} and Ni^{3+} which compare reasonably well with the reported binding energies [24,25]. The absence of a peak at 852.7 ev, which corresponds to Ni^0, may be because the catalyst under study is an unreduced catalyst. In the lower loading nickel is present in the form of Ni_2O_3 and in the higher loadings nickel is present in the form of NiO, Ni_2O_3. Fig. 6 shows the peaks due to Nb $3d_{5/2}$ with two peak maxima E_b = 207.1, 209.9, which compare reasonably well with the reported binding energies of Nb^0, NbO, Nb_2O_5. For all the catalyst samples the amount of surface nickel was estimated from the XPS results. The Ni/Nb surface atomic ratios are depicted in Table 2 and Fig. 7. The surface Ni/Nb ratio increases marginally up to 10 wt.% but there is a drastic increase in the 15 wt.% catalyst sample. However from hydrogen chemisorption results we

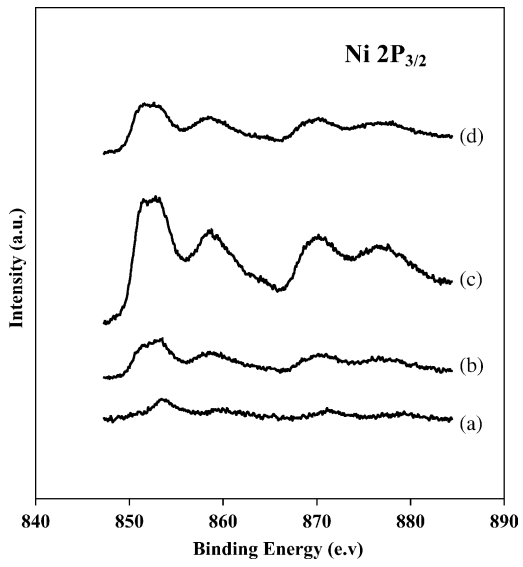

Fig. 5. XPS profiles of Ni $2p_{3/2}$ (a) 2 wt.% Ni/Nb_2O_5, (b) 6 wt.% Ni/Nb_2O_5, (c) 10 wt.% Ni/Nb_2O_5 and (d) 15 wt.% Ni/Nb_2O_5.

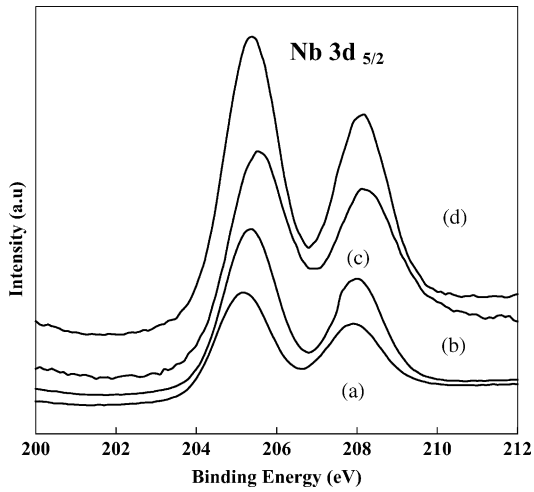

Fig. 6. XPS profiles of Nb $3d_{5/2}$ (a) 2 wt.% Ni/Nb_2O_5, (b) 6 wt.% Ni/Nb_2O_5, (c) 10 wt.% Ni/Nb_2O_5 and (d) 15 wt.% Ni/Nb_2O_5.

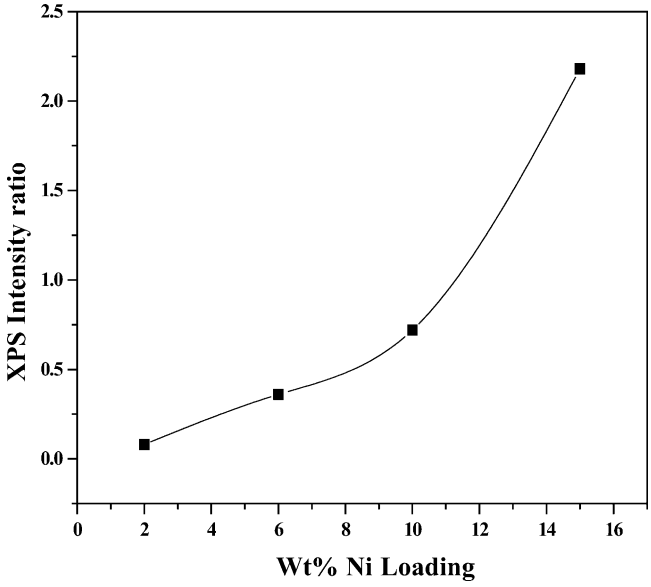

Fig. 7. Relation between XPS intensity ratio Ni/Nb vs. nickel loading.

Table 2
Results of X-ray photoelectron spectroscopy of various Ni/Nb_2O_5 catalysts

wt.% of nickel/niobia	Position and FWHM of Nb $3d_{5/2}$	Position and FWHM of Ni $2p_{3/2}$	XPS intensity I_{Ni} /I_{Nb}
2	207.1(1.45)	856.1(4.09)	0.08
6	207.2(1.43)	855.1(3.30)	0.36
10	207.5(1.55)	854.9(3.27)	0.72
15	207.3(1.46)	854.7(3.23)	2.18

Table 3
Activity results of hydrodechlorination of 1,2,4-trichlorobenzene on Ni/Nb_2O_5 catalysts

wt.% of Ni/Nb_2O_5	% Conversion	Selectivity (%)			
		Benzene	Chlorobenzene	*o*-DCB	*p*-DCB
2.0	42	11	17	36	36
6.0	63	18	6	50	26
10.0	55	12	2	60	26
15.0	45	13	3	56	28

Reaction temperature = 523 K, space velocity = 50,205 h^{-1}, *o*-DCB = *ortho*-dichlorobenzene, *p*-DCB= *para*-dichlorobenzene.

see a reverse trend this may be due to the difference in the pretreatment conditions used in the hydrogen chemisorption and XPS studies or there may however, be a difference in the growth of the crystal shapes that give this unusual effect as the nickel loading increases.

4.7. Catalytic activity

The effect of Ni loading in these catalysts on the hydrodechlorination of 1,2,4-trichlorobenzene at 523 K is shown in Table 3. This table shows the conversion of 1,2,4-trichlorobenzene and selectivities towards benzene, chlorobenzene and dichlorobenzene (including isomers) during hydrodechlorination of 1,2,4-trichlorobenzene between 523 and 613 K. No other reaction products were observed like cyclohexane, chlorocyclohexane or *meta*-dichlorobenzene were detected as was the case with Rh, Pt and Pd catalysts [26–28]. The fact that *meta*-dichlorobenzene was not observed and more *ortho*-dichlorobenzene was formed than *para*-dichlorobenzenes might be attributed to the inductive and steric effects, which form the $Phcl_n$ bonds as proposed by Coq et al. [28] derived from the rate equations used for Pd catalysts. At higher temperatures conversions and benzene selectivity is high. The conversion of 1,2,4-trichlorobenzene depends on the nickel content. Shin et al. [22] reported that conversions depend not only on the surface metal area but also on the amount of spilt over hydrogen, which being hydrogenolytic in nature is responsible for promoting hydrodechlorination activity. A gradual decrease in the catalytic activity was observed with reaction time due to formation of HCl, which poisons the active sites [26,10]. For nickel catalysts, this poisoning effect is stronger at low reaction temperatures (<423 K) [3] producing total deactivation after formation of $NiCl_2$ at the nickel surface. However at temperatures higher than 423 K this poisoning effect is reversible and the metal surface can be maintained partially active by hydrogen during the reaction. It is obvious that there is competition between both the poisoning and the regeneration reactions at any reaction temperature [28,30]. The results of our present study on Ni/Nb_2O_5 have been compared with hydrodechlorination of 1,2,4-trichlorobenzene over Ni/Al_2O_3 catalyst reported by Cesteros et al. [1]. It was found that the Ni/Nb_2O_5 catalysts used in the present study are more efficient than the Ni/Al_2O_3 catalysts.

Fig. 8 shows the relation between TOF (number of molecules of 1,2,4-trichlorobenzene converted per second per site) and nickel loading where TOF is found to be the highest for 6 wt.% Ni/Nb_2O_5. This clearly demonstrates that the conversion of 1,2,4-trichlorobenzene is directly related to the total amount of hydrogen adsorbed on the nickel surface. The 6 wt.% Ni sample exhibited higher activity than other Ni/Nb_2O_5 samples. This is attributed to two factors, that is,

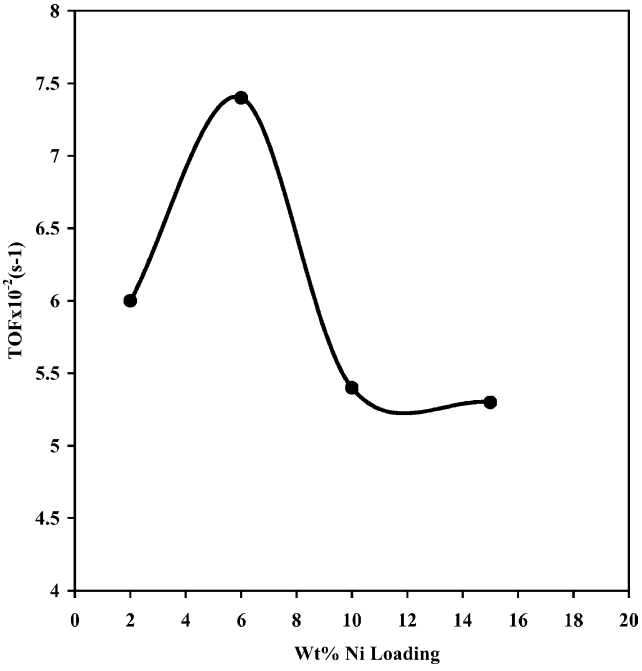

Fig. 8. Relation between turnover frequency (TOF) values (s^{-1}) vs. wt.% Ni loading on niobia.

Table 4
Effect of feed rate on the niobia supported nickel catalysts for the hydrodechlorination of 1,2,4-trichlorobenzene

Feed rate (ml h^{-1})	% Conversion	Selectivity (%)			
		Benzene	Chlorobenzene	*o*-DCB	*p*-DCB
0.4	63	26	6	50	18
0.5	45	28	13	31	28
0.7	49	30	2	20	48
1.0	37	29	19	30	22
1.5	35	23	16	29	32

Catalyst = 6 wt.% Ni/Nb_2O_5, reaction temperature = 523 K, space velocity = 50,205 h^{-1}, *o*-DCB = *ortho*-dichlorobenzene, *p*-DCB= *para*-dichlorobenzene.

Table 5
Effect of temperature on the niobia supported nickel catalysts for the hydrodechlorination of 1,2,4-trichlorobenzene

Reaction temperature (K)	% Conversion	Selectivity (%)			
		Benzene	Chlorobenzene	*o*-DCB	*p*-DCB
523	64	17	6	50	27
553	70	11	14	53	22
583	78	25	17	48	10
613	70	35	37	17	11

Catalyst = 6 wt.% Ni/Nb_2O_5, space velocity = 50,205 h^{-1}, *o*-DCB = *ortho*-dichlorobenzene, *p*-DCB= *para*-dichlorobenzene.

Table 6
Effect of hydrogen flow on the niobia supported nickel catalysts for the hydrodechlorination of 1,2,4-trichlorobenzene

H_2 flow rate (l h^{-1})	% Conversion	Selectivity (%)			
		Benzene	Chlorobenzene	*o*-DCB	*p*-DCB
3.67	23	7	7	60	26
6.13	27	5	9	57	29
8.58	37	15	9	49	27
11.0	63	26	6	50	18

Catalyst = 6 wt.% Ni/Nb_2O_5, reaction temperature = 523 K, space velocity = 50,205 h^{-1}, *o*-DCB = *ortho*-dichlorobenzene, *p*-DCB= *para*-dichlorobenzene.

to the higher intrinsic activity (TOF) and to the greater number of active nickel sites as the hydrogen pulse chemisorption technique showed in Table 1. Dispersion measurements showed that the 6 wt.% Ni catalyst exhibited the highest intrinsic activity (activity per site). The decrease of TOF at higher loading is attributed to the presence of larger crystallites of nickel as evidenced from hydrogen uptake and XRD results.

4.8. Mass transfer

The mass transfer limitations in the hydrodechlorination of 1,2,4-trichlorobenzene are estimated by plotting a graph of conversion as a function of catalyst weight. A linear relationship would indicate the absence of any diffusion limitations during the reaction [29,30]. The results presented in the Fig. 9 indicate that the resistance to mass transfer is negligible.

4.9. Effect of feed rate

The results presented in Table 4 shows the effect of feed rate on the conversion of 1,2,4-trichlorobenzene. The feed rate was varied from 0.4 to 1.5 ml h^{-1}. The major product was *o*-dichlorobenzene. The conversion was found to decrease as the feed rate increased. The selectivity towards the formation of benzene also decreased with the increase in the feed rate. A 10% decrease in conversion is noticed as the feed rate varied from 0.4 to 1.5 ml h^{-1}. This indicates

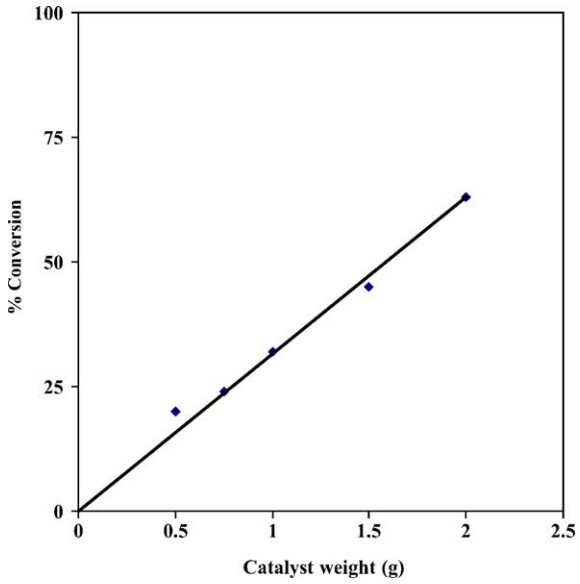

Fig. 9. Relation between catalyst weight and % conversion of 6 wt.% Ni/Nb_2O_5.

that high hydrogen flow rates and low feed rates favour the hydrodechlorination of 1,2,4-trichlorobenzene.

4.10. Effect of temperature

The results presented in the Table 5 shows the effect of temperature on the conversion and selectivity with the reaction of 1,2,4-trichlorobenzene. The conversion of 1,2,4-trichlorobenzene is found to increase with increase in temperature but is maximum at a temperature of 583 K. The selectivity towards the formation of benzene increased with increase in the temperature. There is a 10% increase in conversion as the temperature is varied from 523 to 583 K and there is a decrease in conversion at 613 K.

4.11. Effect of hydrogen flow rates

The effect of hydrogen flow on the hydrodechlorination was studied by carrying out the reactions in the hydrogen concentration range of 3.6 to 11.0 l h^{-1} shown in Table 6. The conversion of 1,2,4-trichlorobenzene increased from 23 to 63% with increase in hydrogen flow. The selectivity for benzene increased from 7 to 26% when the hydrogen flow was increased from 3.6 to 11.0 l h^{-1}.

5. Conclusions

1. Several Ni/Nb_2O_5 catalyst samples have been prepared and characterized by XRD; BET areas, SEM, TPD, TPR and hydrogen chemisorption techniques. These catalysts were tested in the hydrodechlorination of 1,2,4-trichlorobenzene in the vapour phase.
2. The powder XRD detects the peaks corresponding to nickel oxide and T-phase of niobia.
3. SEM micrographs detect the presence of homogeneous nickel oxide particles in the range of 3000–5000 Å.
4. In TPR the amount of hydrogen consumed for the reduction of the nickel exceeded the theoretical value due to spillover of hydrogen from the metal to the support. The shift of T_{max} values with nickel loading might be due to the existence of strong metal support interaction.
5. In TPD the low temperature region below 625 K has been associated with different adsorption states of the hydrogen (presumably related to a different morphology and size of the nickel particles).
6. In XPS the surface nickel/niobia ratio increases marginally up to 10 wt.% but there is a drastic increase in the 15 wt.% catalyst sample. However from hydrogen chemisorption results we see a reverse trend this may be due to the difference in the pretreatment conditions used in the hydrogen chemisorption and XPS studies or there may however, be a difference in the growth of the crystal shapes that give this unusual effect as the nickel loading increases.
7. The 6 wt.% Ni sample exhibited higher activity than other Ni/Nb_2O_5 samples. This is attributed to two factors, that is, to the higher intrinsic activity (TOF) and to the greater number of active nickel sites as the hydrogen pulse chemisorption technique showed.
8. Thus niobia supported nickel catalysts were found to be highly active for partial hydrodechlorination of 1,2,4-trichlorobenzene. The hydrogen spillover is high in 6 wt.% Ni/Nb_2O_5 due to optimum support interaction with the metal. This was found to be a favourable environment for hydrogen to show higher hydrodechlorination activity.

Acknowledgements

The authors are grateful to Department of Science and Technology (DST), New Delhi and British Council Division, New Delhi for funding under the UK–India Science and Technology Research Fund (UISTRF). We also thank CBMM, Brazil for providing hydrated niobia sample. KSL thanks CSIR for the award of Senior Research Fellowship.

References

[1] Y. Cesteros, P. Salagre, F. Medina, J.E. Sueiras, Appl. Catal. B: Environ. 22 (1999) 135.
[2] Y. Cesteros, P. Salagre, F. Medina, J.E. Sueiras, Appl. Catal. B: Environ. 25 (2000) 213.
[3] Y. Cesteros, P. Salagre, F. Medina, J.E. Sueiras, Appl. Catal. B: Environ. 32 (2001) 25.
[4] A. Converti, M. Zilli, D.M. DeFaveri, G. Ferraiola, J. Hazard. Mater. 27 (1991) 127.
[5] S. Kovenklioglu, V. Cao, D. Shah, R.J. Farrauto, E.N. Balko, AIChE J. 38 (1992) 1003.
[6] I. Nowak, M. Ziolek, Chem. Rev. 99 (1999) 3603.
[7] T. Fung, J. Am. Chem. Soc. 100 (1978) 170.
[8] E.I. Ko, J.M. Hupp, F.H. Rogan, N.J. Wagner, J. Catal. 84 (1983) 85.
[9] E.I. Ko, J.M. Hupp, N.J. Wagner, J. Catal. 86 (1984) 315.
[10] J. Estelle, J. Ruz, Y. Cesteros, R. Fernandez, P. Salagre, F. Medina, J.E. Sueiras, J. Chem. Soc. Faraday Trans. 9215 (1996) 2811.
[11] K.V.R. Chary, G. Kishan, K. Sri Lakshmi, K. Ramesh, Langmuir 16 (2000) 7192.
[12] E.I. Ko, J.G. Weissman, Catal. Today 8 (1990) 27.
[13] D. Bianchi, G.E.E. Gardes, G.M. Pajonk, S.J. Teichner, J. Catal. 38 (1975) 135–146.
[14] G.E. Batley, A. Ekstom, P.A. Johnson, J. Catal. 34 (1974) 368.
[15] W.C. Conner Jr., J.L. Falconer, Chem. Rev. 95 (1995) 759.
[16] G.E.E. Gardes, G.M. Pajonk, S.J. Teichner, J. Catal. 33 (1974) 145.
[17] G.M. Pajonk, S.J. Teichner, J. Bull. Soc. Chem. (1971) 3847.
[18] M.A. Keane, Can. J. Chem. 729 (1994) 372.
[19] Kramer, M. Andre, J. Catal. 58 (1979) 287.
[20] Y. Ikushima, M. Arai, Y. Nishiyama, Appl. Catal. 11 (1984) 305.
[21] Smeds, T. Salmi, L.P. Lindfors, O. Krause, Appl. Catal. A: Gen. 144 (1996) 177.
[22] J. Shin, A. Spiller, G. Tavoularis, M.A. Keane, PCCP 1 (1999) 3173.
[23] Z. Paal, P.G. Menon, Catal. Rev-Sci. Eng. 25 (1983) 141.

[24] S. Narayanan, Zeolites 4 (1984) 231.
[25] P. Salagre, J.L.G. Fierro, F. Medina, J.E. Sueiras, J. Mol. Catal. 106 (1996) 125.
[26] B. Coq, G. Ferrat, F. Figueras, J. Catal. 101 (1986) 434.
[27] N. Balko, E. Prybylski, F. von Trentini, Appl. Catal., B: Environ. 2 (1993) 1.
[28] B. Coq, F. Figueras, P. Bodnariuk, in: F. Cossio, O. Bermudez, G. del Angel, R. Gomez (Eds.), Proceedings of the XI Symposium. Iberoamericano de catalisis, Guanajuato Mexico, June 1988, p. 1145.
[29] W.D. Bossaert, D.E. De Vos, W.M. Van Rhijn, J. Bullen, P.J. Grobet, P.A. Jacobs, J. Catal. 182 (1999) 156.
[30] S. Kumar, S.Z. Hussain, Chem. Eng. Sci. 35 (1980) 1425.